

Definition of seismic vulnerability maps for civil protection systems: The case of lampedusa Island

*Original*

Definition of seismic vulnerability maps for civil protection systems: The case of lampedusa Island / Asteris, Panagiotis G; Cavaleri, Liborio; DI TRAPANI, Fabio; Macaluso, Giuseppe; Scaduto, Gaia. - In: THE OPEN CONSTRUCTION & BUILDING TECHNOLOGY JOURNAL. - ISSN 1874-8368. - ELETTRONICO. - 10:Suppl 1: M5(2016), pp. 87-105. [10.2174/1874836801610010087]

*Availability:*

This version is available at: 11583/2672973 since: 2017-05-25T23:07:13Z

*Publisher:*

Bentham Science Publishers B.V.

*Published*

DOI:10.2174/1874836801610010087

*Terms of use:*

openAccess

This article is made available under terms and conditions as specified in the corresponding bibliographic description in the repository

*Publisher copyright*

(Article begins on next page)



# The Open Construction and Building Technology Journal

Content list available at: [www.benthamopen.com/TOBCTJ/](http://www.benthamopen.com/TOBCTJ/)

DOI: 10.2174/1874836801610010087



## Definition of Seismic Vulnerability Maps for Civil Protection Systems: The Case of Lampedusa Island

Panagiotis G. Asteris<sup>1</sup>, Liborio Cavaleri<sup>2,\*</sup>, Fabio Di. Trapani<sup>2</sup>, Giuseppe Macaluso<sup>2</sup> and Gaia Scaduto<sup>2</sup>

<sup>1</sup> Computational Mechanics Laboratory, School of Pedagogical & Technological Education, Heraklion, GR 14121 Athens, Greece

<sup>2</sup> Department of Civil, Environmental, Aerospace and Materials Engineering (DICAM), University of Palermo, 90128 Viale delle Scienze, Palermo, Italy

**Abstract:** The opportunity to locate and quantify the major criticalities associated to natural catastrophic events on a territory allows to plan adequate strategies and interventions by civil protection bodies involved in local and international emergencies. Seismic risk depends, most of all, on the vulnerability of buildings belonging to the urban areas. For this reason, the definition, by a deep analysis of the territory, of instruments identifying and locating vulnerability, largely favours the activities of institutions appointed to safeguard the safety of citizens. This paper proposes a procedure for the definition of vulnerability maps in terms of vulnerability indexes and critical peak ground accelerations for mid-small urban centres belonging to Mediterranean areas. The procedure, tested on the city centre of the Island of Lampedusa, is based on a preliminary historical investigation of the urban area and of the main formal and technological features of buildings involved. Moreover, the vulnerability of the constructions is evaluated by fast assessment methods (filling of evaluation forms). The vulnerability model, allowing the definition of the fragility curves, is calibrated on the basis of the results of an identification process of prototype buildings, selected to be adequately representative. Their characterizations have been provided using the results of an experimental dynamic investigation to develop high representative numerical model. Critical PGA values have been determined by pushover analyses. The results presented provided an unambiguous representation of the major criticalities with respect to seismic vulnerability and risk, of the city centre of the island, being a suitable tool for planning and handling of emergencies.

**Keywords:** Masonry, PGA, pushover, seismic risk, vulnerability assessment.

### 1. INTRODUCTION

Seismic and hydro-geological risks constitute the major component of the activities involving assistance actions carried out by civil protection bodies because of their repetitiveness and the amount of human resources needed to deal with emergencies. The possibility of coordinated actions and cooperation between different countries comprise an element of fundamental importance, especially if the procedures are based on standardized rules and civil protection plans are characterized by detailed knowledge of the territory and of the possible risks.

The promptness of the response of the organizations involved in emergency management is essential to the success of the operations. This essential feature is achievable by practice (hands-on) exercises aimed to implement a responsiveness system to emergencies, and *via* a deep understanding of the existing risks and the major exposure recognized for the urbanized contexts.

The challenge for the assessment of seismic vulnerability of buildings has been addressed by several researchers who, based on the post processing of data coming from the observation of damaged buildings, proposed simplified

\* Address correspondence to this author at the Department of Civil, Environmental, Aerospace and Materials Engineering (DICAM), University of Palermo, 90128 Viale delle Scienze, Palermo, Italy; Tel: +39 091 23896733; Fax: +39 091 6657749; E-mail: [liborio.cavaleri@unipa.it](mailto:liborio.cavaleri@unipa.it)

relationship linking a vulnerability index with the intensity of a seismic event (Benedettini and Petrini (1984) [1], Braga *et al.* (1984) [2], Angeletti *et al.* (1988) [3], Casolo *et al.* (1993) [4]. In other studies, the interest has been addressed to the definition of fast assessment methods for the vulnerability index and the relative large scale application (Martinelli *et al.* (1999) [5], Dolce *et al.* (2004) [6], Dolce and Moroni (2005) [7], Dolce and Martinelli (2005) [8], Asteris (2008) [9], Asteris *et al.* (2014) [10]. This paper presents the outputs of the activity carried out within the research project “SIMIT-Development of an integrated cross-border Italian-Maltese civil protection network” with specific reference to the assessment of the seismic vulnerability of buildings and definition of vulnerability maps in terms of the vulnerability index and the peak ground acceleration limit values. The usefulness of such a kind of outputs relies on the possibility to operate on a territorial scale for planning civil protection activities under seismic emergencies having a deep knowledge of the risk scenarios. In agreement with the scope of this paper, the criteria adopted for the assessment of vulnerability and definition of the vulnerability maps have been calibrated to provide reliable predictions for typically small urban contexts, which are largely widespread in the Mediterranean areas. The representative test site selected for the activities has been the city centre of the island of Lampedusa. The choice was particularly suitable for the prefixed purposes because of the opportunity to operate on a large quantity of buildings concentrated in a small area with and characterized by a repetitiveness of the constructive typology.

The research activity carried out on the island has been divided in 4 phases, characterized by a progressive level of depth of the analysis, listed below:

- Phase 1: Historical, critical, and typological analysis of the urban centre and typical buildings.
- Phase 2: Simplified assessment of seismic vulnerability of buildings by standard vulnerability forms.
- Phase 3: Choice and validation of a vulnerability model.
- Phase 4: Definition of fragility functions and vulnerability maps.

The historical critical study was aimed at the recognition of the urban evolution of the city centre of Lampedusa over the time and of the regulations succeeded which have changed the constructive and typological framework of buildings. The subsequent typological analysis of the buildings, performed through several surveys, made it possible to categorize the recurring structural types within the city centre of the island and their similarities and differences in relation to periods of construction. Such preliminary activities permit to collect fundamental information, necessary for a fast and effective assessment of the buildings vulnerability. The latter was carried out by the use of evaluation forms, well documented in the literature and commonly used in Italy for the fast assessment of the vulnerability single buildings and building aggregates. The major output coming from the use of vulnerability evaluation forms the estimation of a numerical vulnerability index, suitable to be adopted for the definition of the vulnerability maps.

The definition of fragility curves, which provide a relationship between the intensity of the seismic event (synthetically represented by the Peak Ground Acceleration) and the structural damage, passes through a preliminary calibration which is necessary to adapt the vulnerability model (index of vulnerability vs. PGA) to the characteristic building context. In the current study, the calibration operations have been performed by an experimental dynamic monitoring campaign on two prototype buildings, followed by the realization of the numerical structural models consistent with the experimental results. The seismic assessment of the prototype buildings by static pushover analysis made possible the determination of the critical PGA values to be linked with indexes of vulnerability previously evaluated, in order to adapt the vulnerability model to the urban context of the island of Lampedusa. The final outputs are the fragility curves and the associated vulnerability maps for the urban area of Lampedusa, presented in terms of index of vulnerability and critical peak ground accelerations. A summary of the followed procedure is reported in the scheme of Fig. (1).

## 2. HISTORICAL URBAN EVOLUTION AND TYPOLOGICAL ANALYSIS OF BUILDINGS

The study of the urban evolution represents an important basis for the all the operations aimed at the recognition of building typologies and constructive technologies. It allows to localize within the timeline the historical events, facts, laws and technical prescriptions influencing the constructive practice trends of specific epochs. Lampedusa is a small island situated in the middle of Mediterranean sea (Fig. 2a, b). The evolution of the urban settlement of Lampedusa is concentrated in port area, the seat of trade, tourism and fishing activities (Fig. 2c).

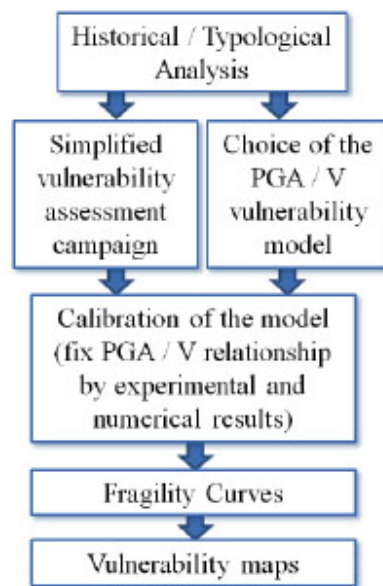


**Fig. (1).** Scheme of the proposed procedure.

The Bourbon colonization of the island started around 1843. Since it was necessary to give accommodation to 120 people arrived to start the settlement and cultivation of the island, it was initiated the construction of the so-called "seven palaces", aligned on a main road axis, and five other buildings on a second line parallel to the first. Approximately in 1845, the construction of 90 buildings as residence for the new settlers was launched. At the end of Bourbon colonization the city centre had a well-defined conformation, but was interested by a new strong growth (1950-1970) because of the increase of tourist flows. Following the construction of the airport (1968), the links with the mainland became much more stable having as effect a further rapid expansion up to the present day. A comparison between the configuration of the old town in 1945, 1970, and up to the current zoning is reported in Fig. (3).

An accurate preliminary analysis of the building typologies in the urban settlement has been also carried out in order to select the most suitable tools for the assessment of the seismic vulnerability at large scale. This allows getting a framework for the classification of buildings, necessary to facilitate the operations of survey and collection of information. The opportunity to take advantage of a preliminary study aimed to associate building typologies and details to certain historical periods, greatly simplified the procedure and allowed a smaller margin of error. From an early examination on the structural types, it resulted that over 85% of the buildings in the area of the city centre had masonry primary structure. The remaining 15% were reinforced concrete buildings or in a few cases had mixed primary structure. The large prevalence of masonry buildings was due primarily to the availability of natural resources on the island which had a rich geological formation of limestone rock in the subsoil. The primary material came directly from the quarries for many years and up to 1970, when two factories for the production of concrete blocks were opened with a consequent change of trend in the choice of the basic building material. Some pictures of typical calcarenite and calcarenite block masonry buildings are reported in Fig. (4).

The quality of the construction and resistant systems was subject to a careful analysis aimed at the characterization of some technological aspects really influent for the recognition of vulnerability. As first it was observed that the majority of the buildings did not exceed two floors above the ground. The walls were typically compact with an adequate thickness. These two elements allowed presuming that in general the stress rate of materials is quite low and the primary structures are generally under safety conditions at least with respect to gravity loads. The reduced height of the buildings also limits the extent of the possible seismic involvement of structures. The primary structural elements, despite a regular degradation due to the aging, presented construction details of good workmanship. The floors were made of RC slabs (or mixed RC-clay block) granting a rigid behavior. It was also recognized that both limestone and concrete block masonries were featured by RC curbs at each level (Fig. 4a, c) and the orthogonal walls resulted effectively clamped at the corners, ensuring a box-like behavior of the structure (Fig. 4a, c). Finally, the walls did not typically exhibit signs of structural instability. On the other hand in most of the cases, the buildings had the configuration of aggregates. The overall configuration presented substantial height differences of the structural bodies,



causing lateral stiffness and strength variations from one floor to the upper one Fig. (5). Such an irregular condition over the height was recognized as the primary and most relevant element of vulnerability for the buildings belonging to the urban area.



**Fig. (2).** Localization of Lampedusa Island and its urban centre.



**Fig. (3).** Expansion of the city centre of Lampedusa Island since 1945.



**Fig. (4).** Typical masonry buildings in the urban centre of Lampedusa: (a, b) Calcarene masonry; c) Concrete blocks masonry.



**Fig. (5).** Irregularity in elevation of building aggregates.

### 3. ASSESSMENT OF VULNERABILITY

The assessment of seismic vulnerability has been performed for masonry and reinforced concrete buildings belonging to the city centre of Lampedusa. For sake of brevity, and since RC structures represent a really low portion of

all buildings, the procedure for the assessment described in the following regards only masonry buildings.

The recognition of vulnerability of masonry structures has been carried out using the evaluation forms developed by INGV/GNDT - National Group for the Defence against Earthquakes [11]. In particular, the need to correlate scientific information with on-site surveys has requested the use of so called "second level forms", since their compilation is not direct but requires a deeper investigation of the geometrical and mechanical characteristics, followed by the evaluation of specific parameters by a numerical calculation.

The assessment of the vulnerability by the 2<sup>nd</sup> level GNDT forms is based on the determination of a vulnerability index which is a conventional measure of the propensity of a building to undergo seismic damaging. The index is numerically calculated as sum of vulnerability scores obtained by the analysis of 11 parameters considered fundamental for the identification of the seismic behavior of masonry buildings. The vulnerability index that is obtained allows to compare buildings and to establish graded lists or a map of vulnerability (as in the case of the present study). The choice of GNDT 2<sup>nd</sup> level forms has been basically determined on the basis of the following requirements that have been placed at the base of the research:

- Possibility of detecting pre-earthquake vulnerability.
- Adequate amount of information about the parameters that affect the vulnerability.
- Compilation without specific investigations or detailed surveys on buildings.
- Consolidated use of the forms on the national territory.
- Possible adaptation of the forms to particular needs found in the area.
- Availability of the same type of forms masonry and RC structures.

The GNDT vulnerability assessment form for masonry buildings requires the determination of the 11 parameters reported in Table 1. Each parameter is associated with a class of vulnerability between A and D, where A represents the best condition and D the worst. At the same time a class of quality of the information used to establish the class of vulnerability, is assigned. The vulnerability classes are characterized by increasing scores and identified by the symbol  $c_{vi}$ . The single parameters are moreover weighted by the weight  $p_i$ , which establishes their influence on the overall assessment of the vulnerability. The Table 1 shows the list of the 11 parameters of vulnerability, the scores assigned to the classes and weights. Regarding the weights, the GNDT procedure provides only those relative to the parameters 1, 2, 3, 4, 6, 8, 10 and 11 while the weights of parameters 5, 7 and 9 have been calibrated according to the influence presumed after the general observation of the built. In particular, it was decided to penalize the conditions of irregularity in elevation because of the considerations reported above.

**Table 1. Parameters for the identification of vulnerability of masonry buildings in GNDT forms and related scores and weights.**

Parameter		Class $C_{vi}$				Weight
		A	B	C	D	$p_i$
1	Type and organization of the resisting system	0	5	20	45	1.00
2	Quality of the resisting system	0	5	25	45	0.25
3	Conventional resistance	0	5	25	45	1.50
4	Position of the building and foundations	0	5	15	45	0.75
5	Floors	0	5	25	45	0.75
6	Configuration in plan	0	5	25	45	0.50
7	Configuration in elevation	0	5	25	45	1.75
8	Walls maximum interaxis	0	5	25	45	0.25
9	Roof	0	15	25	45	0.50
10	Non-structural elements	0	0	25	45	0.25
11	Current conditions	0	5	25	45	1.00

The vulnerability index  $V$  is defined as

$$V = \sum_i c_{vi} p_i \quad (1)$$

taking values between 0 and 328.5. More usually the vulnerability index is expressed in cents, therefore a normalized vulnerability index can be expressed as



$$\bar{V} = \frac{V}{382.5} \times 100 \quad (2)$$

The attribution of the vulnerability class depends specifically on each parameter and can be performed by simple observations or may include simplified calculations. In absence of direct experimental information the average shear strength referenced in Italian Code (DM 14.01.2008) [12] were adopted. For sake of brevity a complete description of the GNDT criteria for the attribution of the scores will not be included in the text.

The operations of vulnerability recognition involved an area comprising almost all of the buildings in the city centre. The extension of the area investigated is reported in Fig. (6). The survey involved 288 individual buildings or building aggregates. The main data are summarized in Table 2.

**Table 2. Buildings involved in the investigation.**

Total buildings	Masonry buildings	Reinforced concrete buildings
288	264	24
	91.7%	8.3%

Regarding to masonry buildings a statistical output is observable in Fig. (7), where the probabilistic distribution of the normalized vulnerability index recognized is represented. It appears clear that the vulnerability was settled to low-mid levels. The average normalized vulnerability index was 25.30 while the maximum did not exceed 50. The recorded distribution showed however a wide variance.

#### 4. CALIBRATION OF THE VULNERABILITY MODEL FOR THE DEFINITION OF FRAGILITY CURVES

The definition of a relationship between the severity of the earthquake and the damage, through the vulnerability index  $V$ , is based on the observation that a building, subject to seismic actions of increasing severity is typically characterized by a beginning stage of damaging, a phase of increase and a rapid decay up to the collapse. If one assumes the parameter  $y=a/g$ , which identifies the normalized ground acceleration, as index of the severity and the parameter  $D$  as index of the damage (between 0 and 1), identifying the loss of the economic value, the relationship may be represented by a fragility function Fig. (8).



**Fig. (6).** Building aggregates involved in the assessment of the vulnerability.

On this curve one can identify the accelerations corresponding to damage beginning  $y_i$  and collapse  $y_c$ . As proposed in Guagenti and Petrini (1989) [13], a linearized fragility function (Eq. 3) has been used to reduce the problem of establishing the fragility function to the simple calculation of the values of  $y_i$  and  $y_c$ .



$$D(y, V) = \begin{cases} D = (y - y_i) / (y_c - y_i) \\ D = 0 & \text{per } y < y_i \\ D = 1 & \text{per } y > y_c \end{cases} \quad (3)$$

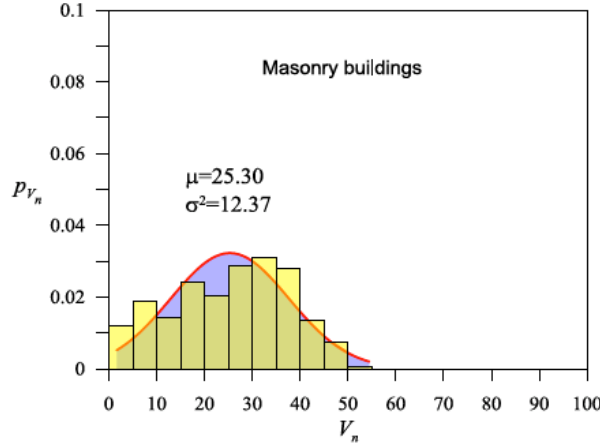


**Fig. (7).** Probabilistic distribution of normalized vulnerability index for masonry buildings detected by GNDT procedure.

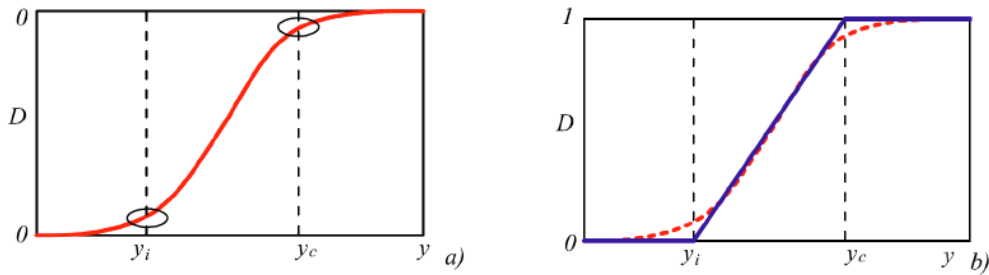


**Fig. (8).** Fragility functions: (a) Fully defined function; (b) Trilinear equivalent function.

In particular it was assumed the functional relationship linking the early damage acceleration  $y_i$  and the collapse acceleration  $y_c$  to the vulnerability index according to [13] is given by the following expressions

$$y_i(V) = \alpha_i \exp[-\beta_i(V)] \quad (4)$$

$$y_c(V) = \alpha_c + \beta_c(V)^\gamma \quad (5)$$

The equations above reported, graphically represented in Fig. (9), depend on the parameters  $\alpha_i$ ,  $\beta_i$ ,  $\alpha_c$ ,  $\beta_c$  and  $\gamma$  whose calibration is of great importance for the reliability of the results and has to be performed by major investigations on typical buildings.

For this reason the calibration has been performed on the basis of an experimental investigation, which included the dynamic identification of 2 prototype buildings chosen to be adequately representative of the previously discussed features of the urban centre built. The final purpose was the definition of refined numerical models to be used for the determination of the critical PGA values ( $y_i$  and  $y_c$ ) at the specific vulnerability levels characterizing the buildings. The calibration process was performed according to the following steps

- Choice of the prototype building and assessment of the vulnerability index by GNDT forms.
- Dynamic identification of the buildings and definition of the numerical models.

- Evaluation of  $y_i$  and  $y_c$  values by static pushover analyses.
- Positioning  $V-y(V)$  points and best fitting.

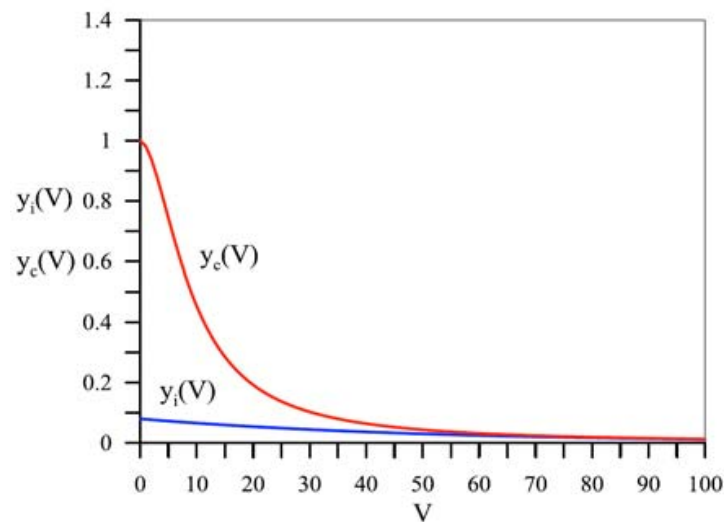


**Fig. (9).** General  $y(V)$  relationships (Guagenti and Petrini (1989)).

The buildings selected for the investigation were the City Hall of Lampedusa (BT “A”), (Fig. 10a) and the headquarters of the Marine Protected Area of Lampedusa (BT “B”), (Fig. 10b). The original drawings of the two structures were available and were checked on site.



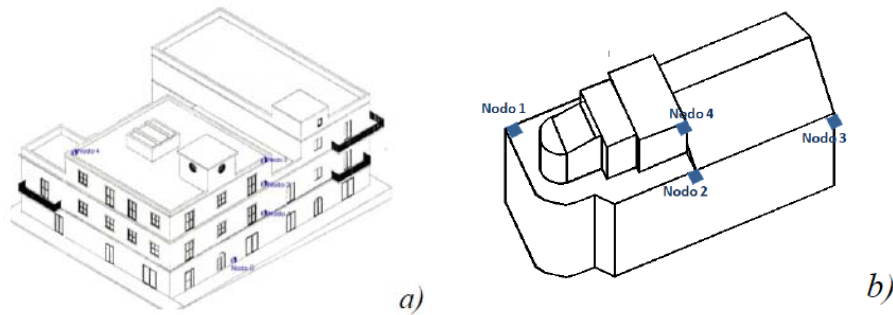
**Fig. (10).** Prototype buildings: (a) City Hall of Lampedusa (BT “A”); (b) Seat of the Marine Protected Area of Lampedusa (BT “B”).

A system of triaxial accelerometers was positioned in both the buildings. The location of the acquisition nodes is reported in Fig. (11).

The analysis of the signal allowed the structural identification and in particular the attribution of the elastic properties to assign to the structural models in order to match the experimentally detected dynamic response in terms of fundamental frequencies. Masonry shear strength and normal compressive strength values adopted were determined by Italian Code [12] indication on the basis of the recognition of masonry typology carried out on site. In particular, for both buildings, calcarenite masonry with regular mortar joints was recognized as recurring masonry typology. For sake of brevity the descriptions and the results reported in the following refer to BT “A” only whose normalized vulnerability index, calculated according to GNDT procedure was  $V=36.29$ . Elastic and mechanical values adopted are reported in Table 3.

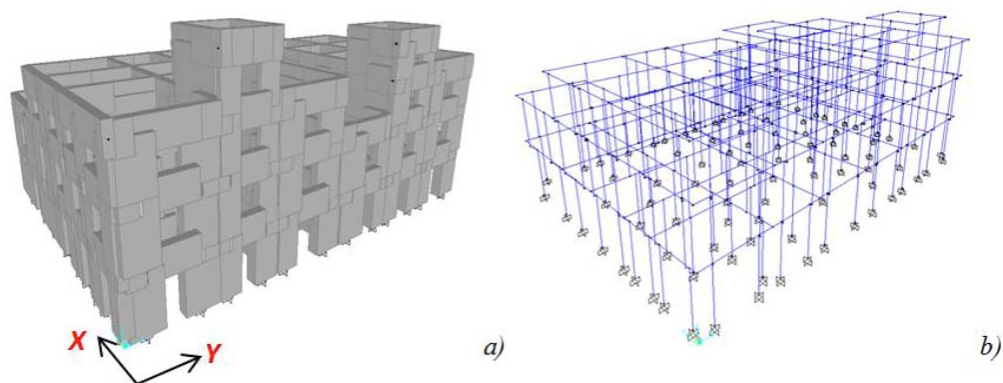
**Table 3. Mechanical features adopted for masonry (BT "A").**

$f_m$	$t$	$E_m$	$G_m$	$w$
$N/cm^2$	$N/cm^2$	$N/mm^2$	$N/mm^2$	$kN/m^3$
190	3,50	1260	420	16

**Fig. (11).** Position of the acquisition nodes: (a) BT"A"; (b) BT"B".

#### 4.1. Numerical Model of BT "A"

Structural model was performed using the software SAP 2000 NL. A "frame-type" schematization of the masonry structure was adopted. Walls were modelled as beam/column elements with reference to their centroidal axis. Taking into account the presence of RC curbs at any level, it was assumed that the coupling masonry beams were flexurally resistant. These latter were modelled as elastic elements with the same material properties used for masonry. The presence of concrete slabs allowed moreover to consider the rigid diaphragm constrain. The loads coming from the floors were distributed linearly on the beams at each level. Finally, the connections at the areas of overlap between the walls and the masonry beams, were modelled as rigid elements. A three-dimensional representation of the model is shown in Fig. (12).

**Fig. (12).** 3D view of the structural model (BT"A"): (a) solid scheme; (b) unifilar scheme.

The introduction of nonlinearities was carried out by the use of  $\tau$ - $\gamma$  (shear-angular sliding) plastic hinges within vertical elements. Considering that for of small displacements the angular sliding of a masonry panel is equal to its interstorey drift  $\delta/h$ , the plastic hinge length was considered as the entire height of the wall (Fig. 13b). Hinges were governed by an elastic - perfectly plastic law (Fig. 13a) characterized by a yielding point in correspondence of the maximum shear stress  $\hat{\sigma}_t$  evaluated according to the expression of Turnšek and Cacovic [14] below reported

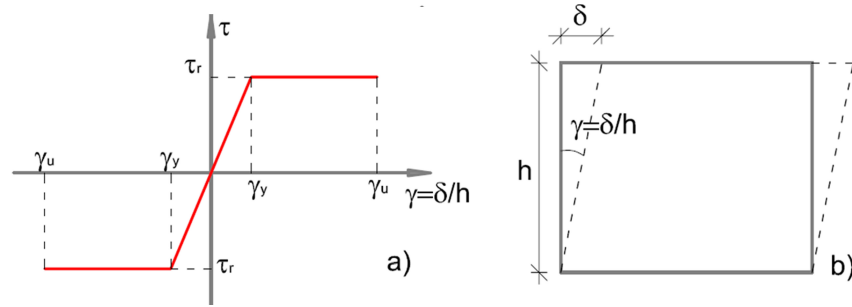


**Fig. (13).** Shear plastic hinges definition: (a) stress-strain law; (b) angular sliding of a generic panel.

$$\tau_r = \frac{1.5\tau_0}{b} \sqrt{1 + \frac{\sigma_0}{1.5\tau_0}} \quad (6)$$

being  $\tau_0$  the shear strength in the absence of vertical loads (as defined in Table 3),  $\sigma_0$  the average compression stress acting on the wall and  $b$  a parameter taking into account the aspect ratio of the wall, varying in the range 1-1.5, and that is assumed to be on average 1.25.

As ultimate drift for the walls it was assumed the value  $\gamma_u = \delta_u / h = 0.004$ , assuggested by the Italian Codes for the life prevention limit state.

#### 4.2. Modal Analysis of BT "A"

The modal analysis of the numerical model identified, revealed a significant irregularity in structural response especially for direction  $X$ , where the participating mass was distributed on the first two modes at frequencies between 3.5 and 4.10 Hz. In direction  $Y$  the third mode had a mass concentration of 55% at the frequency of 5 Hz. The distribution of the participating masses in the first 12 modes in  $X$  and  $Y$  directions is graphically represented in Fig. (14).

The modal shapes associated to the first 3 modes are shown in Fig. (15). In both the 3 modes a significant torsional component can be recognized. The reason can be found observing the variation of the plan conformation from one floor to the upper one, cause of an irregular distribution of masses and stiffness.

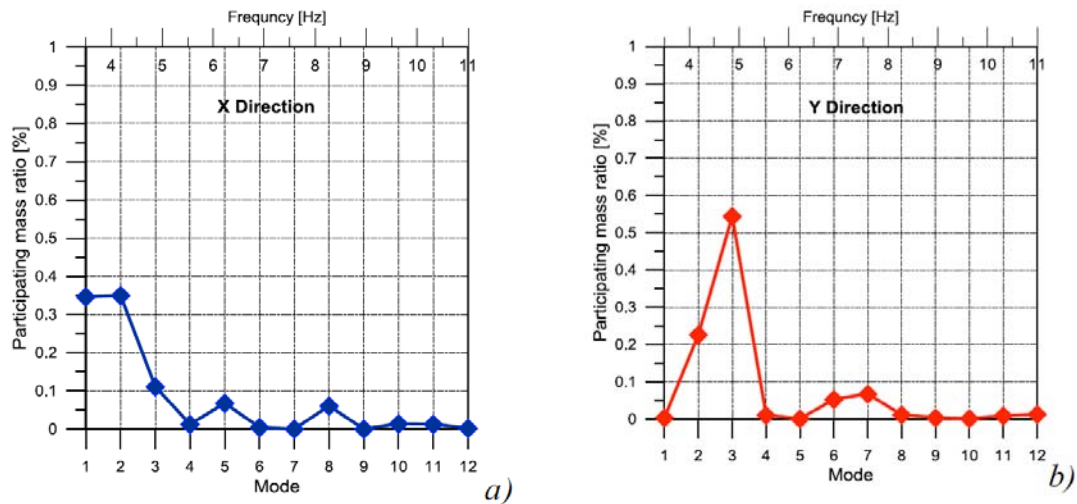
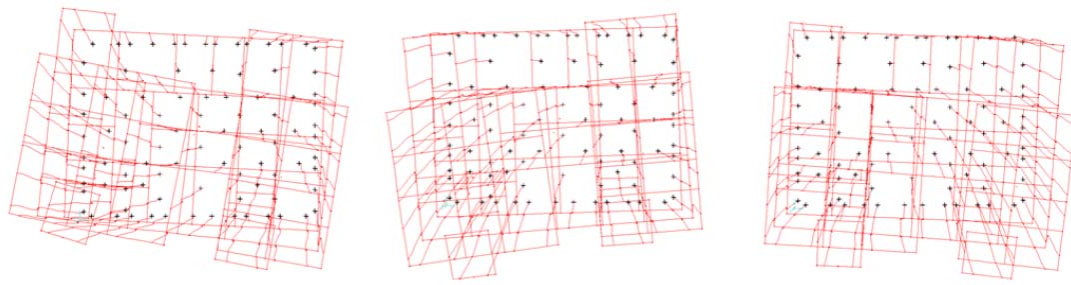


**Fig. (14).** Participating mass within the first 12 modes: (a)  $X$  direction ; (b)  $Y$  direction .





Mode 1:  $T = 0.286$  s;  $f = 3.49$  Hz    Mode 2:  $T = 0.243$  s;  $f = 4.10$  Hz    Mode 3:  $T = 0.237$  s;  $f = 4.21$  Hz

**Fig. (15).** Modal shapes: Modes 1, 2 e 3.

#### 4.3. Pushover Analysis for the Evaluation of Early Damage and Collapse Accelerations

Pushover analysis was carried out in order to define the capacity of the structures especially in terms of early damage and collapse ground accelerations. Given the strategic role of the buildings the elastic response spectrum was defined (according to Italian Code), considering return period of  $T_R = 2475$  years, a spectral amplification factor  $F_o = 3.09$  and stratigraphic amplification coefficient  $S = 1.2$ . In order to consider the uncertainties on the actual response beyond the elastic limit, as well as also suggested by the codes, the pushover analysis was repeated with two force profiles for each direction. A modal distribution and a uniform distribution of lateral loads were considered. Given that the shear hinges introduced were not sensitive to the axial load variation, the profiles were assigned with a single sign for each direction considered. The base shear ( $V$ ) - roof displacement ( $d$ ) responses obtained by the 4 analyses are shown in Fig. (16) for the multi degree of freedom system (MDOF).

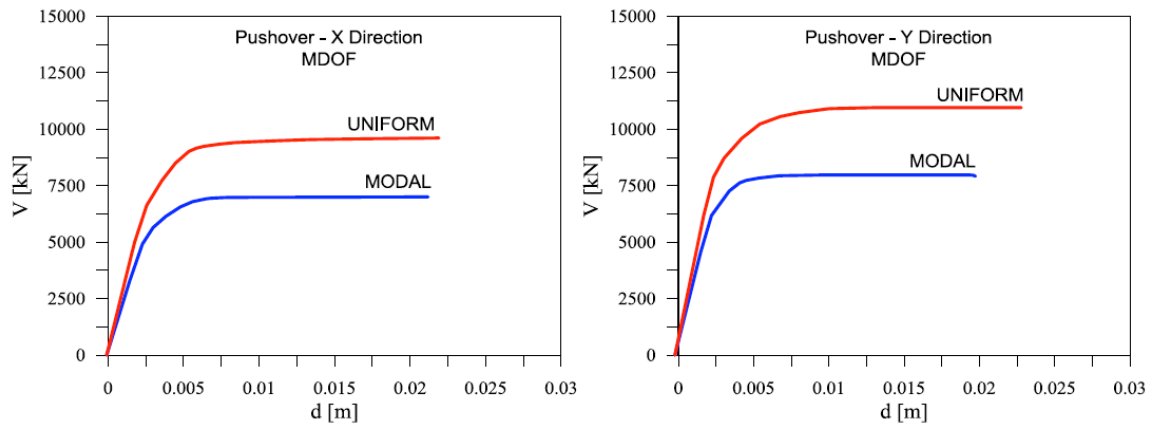


**Fig. (16).** Capacity curves of the MDOF systems.

The curves were reduced to those of the equivalent ( $V^*$  -  $d^*$ ) single degree of freedom system (SDOF) through the well-known following relationships

$$V^* = \frac{V}{\Gamma_1}; \quad d^* = \frac{d}{\Gamma_1} \quad (7)$$

$\Gamma_1$  being the modal participation factor for the predominant mode in the direction considered. The identification of the properties of SDOF is commonly performed associating a bilinear equivalent curve. Mass  $m^*$ , stiffness  $k^*$  and period  $T^*$  of the equivalent SDOFs were therefore calculated as:

$$m^* = \sum_{i=1}^n \Phi_{i1} m_i; \quad k^* = \frac{F_y^*}{d_y^*}; \quad T^* = 2\pi \sqrt{\frac{m^*}{k^*}} \quad (8)$$

and being the yielding force and the yielding displaced identified by the bilinear SDOFs.

For sake of brevity data of bilinear system are not reported in the within the text.

It was firstly verified the capacity of the structure to support the request associated to the earthquake with the reference spectrum for the 4 conditions considered. This test gives an idea about the reliability of the vulnerability index detected by the GNDT procedure and for better comprehension can be performed in the ADSR plane overlapping the constant ductility non nonlinear demand spectrum and the bilinear curve of the SDOF systems. In this way it is possible to evaluate for each SDOF the yield acceleration  $S_{ay}$  and the acceleration  $S_{ae}$  that would be required to an indefinitely elastic system having the same elastic period  $T^*$ , respectively, as:

$$S_{ay} = \frac{F_y^*}{m}; S_{ae} = S_{ae}(T^*) \quad (9)$$

the reduction factors  $q^*$  are thus evaluated as:

$$q^* = \frac{S_{ae}}{S_{ay}} \quad (10)$$

If for all the SDOFs  $T^* < T_c$ , the requested ductility  $\mu_r$  for all of them (each one characterized by  $T^*$  and  $q^*$ ) can be calculated by the expressions of Miranda and Bertero (1993) [15]

$$\mu_r = (q^* - 1) \frac{T_c}{T^*} + 1 \quad (T^* < T_c) \quad (11)$$

The acceleration and displacement components for the non-linear spectrum having the constant ductility  $\mu_r$ , were obtained by the expressions of Vidic *et al.* (1994) [16]).

$$S_a = \frac{S_{ae}}{q(\mu_r, T)}; S_d = \frac{\mu_r}{q(\mu_r, T)} S_{de} = \mu_r \frac{T^2}{4\pi^2} S_a \quad (12)$$

For the 4 cases considered the superposition of the demand spectra of and capacity curves led to the results shown in Fig. (17). It can be noted that the displacements associated with the capacity curves were always greater than the request displacement identified by the performance point. This evidence, appears to be consistent with the mid-low value of vulnerability ( $V=36.29$ ) calculated for the building.

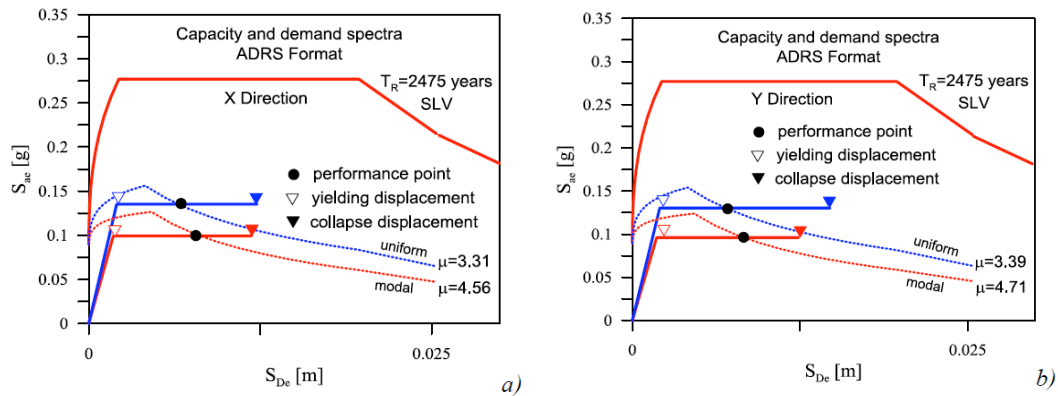
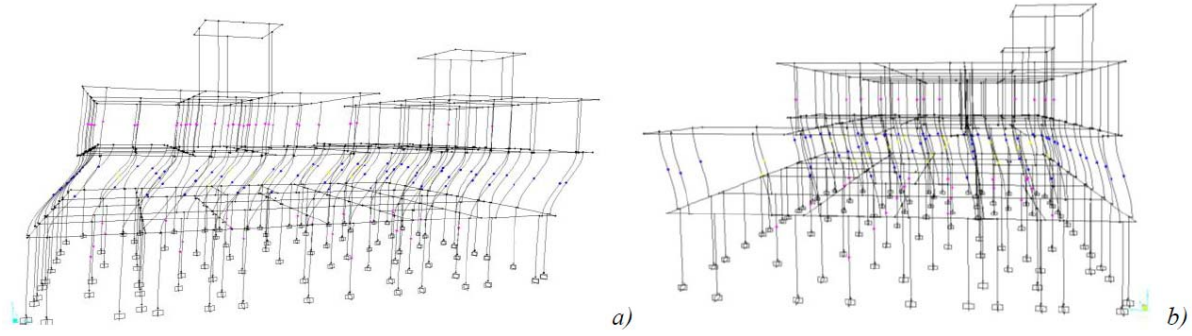


Fig. (17). Capacity and demand spectra in AD format: (a) X Direction; (b) Y Direction.



**Fig. (18).** Major collapse mechanism recognized: (a) X direction; (b) Y direction.

In Fig. (18) the most critical collapse mechanisms detected through the pushover analysis for the directions X and Y are reported. Damage was substantially localized at the first elevation because of the relevant variation of lateral stiffness and resistance that occurs from the ground floor to the upper one. Such a result is consistent to what yet highlighted in section 2 about the high irregularity in elevation of buildings belonging to the city centre of Lampedusa. Moreover it confirms the representativeness of the prototype building selected.

The definition of peak ground accelerations (PGA) corresponding to the beginning of the damage ( $PGA_i=y_i$ ) and collapse ( $PGA_c=y_c$ ). The first condition was associated to the yielding displacement, the second to the collapse displacement both determined on the bilinear curves. The previous expression by Miranda and Bertero, in the case of  $T^* < T_c$ , can be rewritten as

$$d_{r,max}^* = \frac{d_e^*}{q^*} \left[ (q^* - 1) \frac{T_c}{T^*} + 1 \right] \quad T^* < T_c \quad (13)$$

which expresses, for a system characterized by  $q^*$  and  $T^*$ , the relationship between the inelastic displacement  $d_{r,max}^*$  demand and the displacement that would be required for the ideal indefinitely elastic and  $d_e^*$ .

By calculating the reduction factor  $q^* = \tilde{q}^*$ , reduction factor recalculated as function of the actually available ductility  $\mu_d$  as

$$\tilde{q}^* = 1 + (\mu_d - 1) \frac{T^*}{T_c} \quad (T^* < T_c) \quad (14)$$

and fixing the period  $T^*$ , it is possible to calculate the displacements associated to an elastic response spectrum characterized by a different PGA value.

In particular the following values for the ductility corresponding to the early damage and collapse were used for the determination of  $\tilde{q}^*$

$$\mu_{d,y} = 1; \quad \mu_{d,u} = \frac{d_u^*}{d_y^*} \quad (15)$$

The elastic displacement associated to the early damage and collapse elastic spectra are therefore

$$d_{e,y}^* = S_{De,u}(T^*) = \frac{d_y^* \tilde{q}^*}{\left[ (\tilde{q}^* - 1) \frac{T_c}{T^*} + 1 \right]}; \quad d_{e,u}^* = S_{De,u}(T^*) = \frac{d_u^* \tilde{q}^*}{\left[ (\tilde{q}^* - 1) \frac{T_c}{T^*} + 1 \right]} \quad (16)$$

hence the associated spectral accelerations are:

$$S_{ae,y}(T^*) = \frac{4\pi^2}{T^2} S_{De,y}(T^*); \quad S_{ae,u}(T^*) = \frac{4\pi^2}{T^2} S_{De,u}(T^*) \quad (17)$$

Since for all the cases considered resulted  $T_B \leq T^* \leq T_C$ , where the expression of the response spectrum is

$$S_{ae}(T^*) = PGA \times S \times F_0 \quad (18)$$

by substituting the values  $S_{ae,u}(T^*)$  and  $S_{ae,y}(T^*)$  the critical PGA values are finally obtained

$$y_i = PGA_i = \frac{S_{ae,y}(T^*)}{S \times F_0}; \quad y_c = PGA_c = \frac{S_{ae,c}(T^*)}{S \times F_0} \quad (19)$$

The reference  $PGA_c$  and  $PGA_i$  values, calculated for the different load profiles considered, are reported in Table 4 together with the other parameters necessary for their determination.

**Table 4.  $PGA_c$  and  $PGA_i$  values calculated for the considered analyses.**

Collapse PGA (PGAc)							
Direction and load	$d_u^*$ (m)	$\tilde{q}^*$	$T_c$ (s)	$T^*$ (s)	$d_{cu}$ (m)	$Se(T)$ (g)	$y_c=PGA_c$ (g)
DIR X mod	0,0120	3,84	0,529	0,267	0,0069	0,385	0,106
DIR X uni	0,0123	3,28	0,529	0,240	0,0067	0,457	0,126
DIR Y mod	0,0124	3,98	0,529	0,270	0,0072	0,390	0,107
DIR Y uni	0,0147	3,93	0,529	0,250	0,0080	0,507	0,140
Early damage PGA (PGAi)							
Direction and load	$D_y^*$ (m)		$T_c$ (s)	$T^*$ (s)	$d_{ey}$ (m)	$Se(T^*)$ (g)	$y_i=PGA_i$ (g)
DIR X mod	0,0018	1,0	0,529	0,267	0,0018	0,0,99	0,0272
DIR X uni	0,0020	1,0	0,529	0,240	0,0020	1,39	0,0383
DIR Y mod	0,0018	1,0	0,529	0,270	0,0018	0,98	0,0270
DIR Y uni	0,0020	1,0	0,529	0,250	0,0020	1,29	0,0355

#### 4.4. Calibration of the Fragility Curves

Pushover analyses allowed to determine the reference critical accelerations for the prototype buildings BT"A" and BT"B". In particular, reference was made to minimum values respectively for accelerations of early damage and collapse. PGA values are reported in Table 5 together with the values of the respective normalized vulnerability indexes of the buildings.

**Table 5.  $y_c$ ,  $y_i$  and V values calculated of the prototype buildings.**

	V	$y_i$ [g]	$y_c$ [g]
BT"A"	36.29	0.027	0.106
BT"B"	22.10	0.051	0.272

Joining PGA values and vulnerability indexes on a  $V$ - $y$  plane, it is possible to calibrate the coefficients governing the  $y(V)$  relationships according to the model by Guagenti and Petrini (1989), providing suitable general expressions having validity for the buildings of the city centre of Lampedusa (Fig. 19).

The values of coefficients  $\alpha_i$ ,  $\beta_i$ ,  $\alpha_c$ ,  $\beta_c$  and  $\gamma$ , which allowed to achieve the best correspondence between detected and predicted  $V$ - $y(V)$  values, are given in Table 6.

**Table 6. Parameters calibrating the  $y(V)$  relationships for ma-sonry building of the city centre of Lampedusa.**

$\alpha_i$	$\beta_i$	$\alpha_c$	$\beta_c$	$\gamma$
0,0578	0,0210	19,371	0,00123	2,423



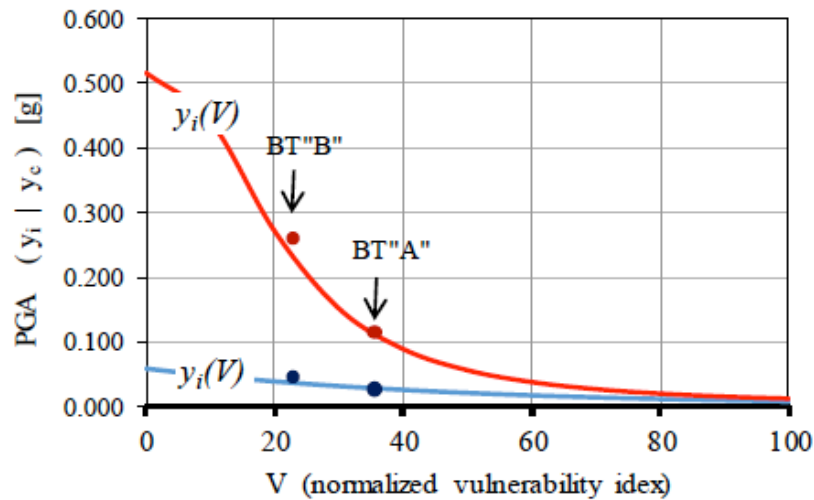


**Fig. (19).** Calibration of the  $y_i(V)$  relationships for the masonry buildings of the city centre of Lampedusa.

Consequently, the fragility functions for masonry buildings of the city centre of Lampedusa are univocally identified for the different vulnerability indexes (Fig. 20). The latter, once known the vulnerability index of a building, allow to determine the level of damage that this will undergo as function of the severity of the earthquake, identified by the peak ground acceleration. This tool is particularly useful for Civil Protection purposes, since it allows to make damage estimations on buildings for given scenarios of seismic intensity as described in the subsequent section.

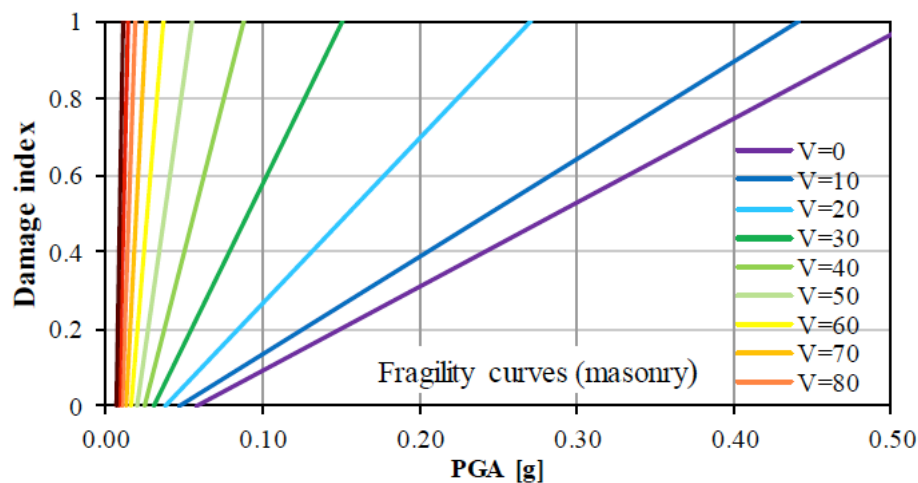


**Fig. (20).** Fragility functions for masonry buildings of the city centre of Lampedusa.

## 5. VULNERABILITY MAPS OF THE CITY CENTRE OF LAMPEDUSA

The final output is reported in 3 maps. The first one (Fig. 21) is the map of the vulnerability index, obtained by the application of the GNDT procedure to the masonry buildings investigated, which represent almost the totality within the urban centre.

The map has a reference chromatic scale of the normalized vulnerability index going from cooler colours (blue - green), associated to a lower vulnerability, to warm colours (red-orange) associated to increasing vulnerability values.

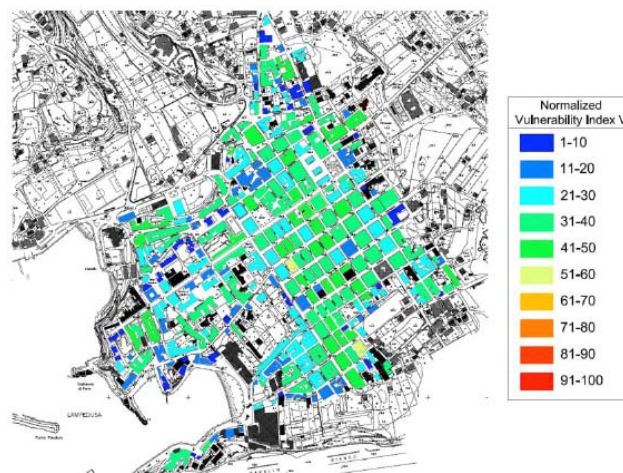


**Fig. (21).** Map of the vulnerability index for the city centre of Lampedusa.

The subsequent two maps, collapse PGA map (Fig. 22) and early damage PGA map (Fig. 23), were obtained substituting the vulnerability indexes relative to each building into Eqs. (4) and (5), where parameters  $\alpha_p$ ,  $\beta_p$ ,  $\alpha_c$ ,  $\beta_c$  and  $\gamma$  were those determined in the previous section. Within these two maps the warmest colours are associated to the lowest values of ground acceleration, representative of the most critical conditions. Looking at the output expressed by the vulnerability index map, the overall condition does not present relevant criticalities. The average vulnerability is settled to mid-low values.

The early damage and collapse PGA values are instead rather low. However, considering the expected PGA values, which are associated the low seismicity of the area, one can exclude, with good approximation, the possibility of the occurrence of catastrophic post-earthquake scenarios. It appears evident from the maps as the areas characterized by a greater vulnerability refer to the oldest urban disposition, that was also the most subject to further transformations during the time. The peripheral areas, consisting of newer buildings, resulted instead less vulnerable, consistently with the expectations coming from the initial assessments.

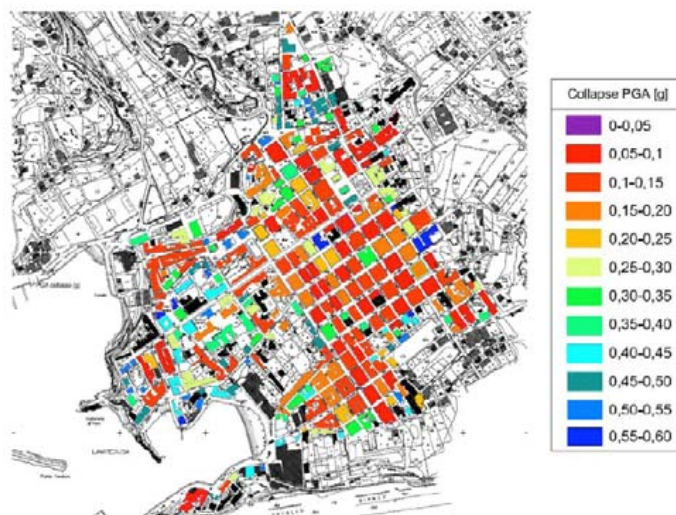


**Fig. (22).** Map of collapse PGA for the city centre of Lampedusa.

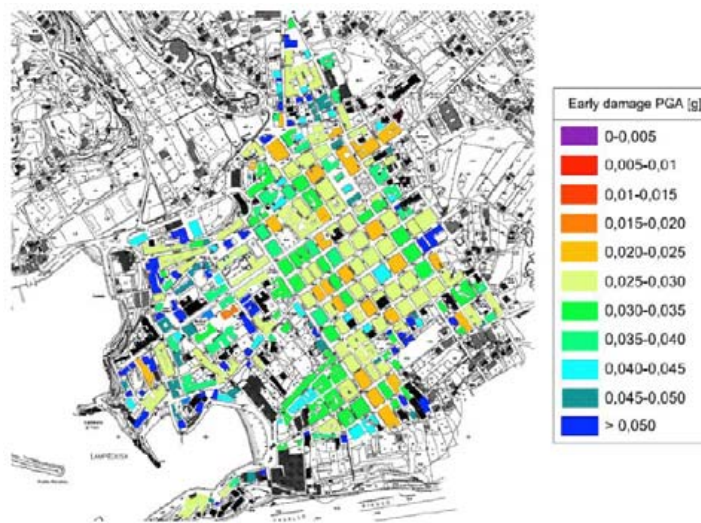


**Fig. (23).** Map of early damage PGA for the city centre of Lampedusa.

## CONCLUSION

This paper presented the methodological procedure and the outcomes of a theoretical/experimental research activity carried out to assess the profile of the seismic vulnerability of the city centre of the Lampedusaisland. The major objective was the definition of seismic vulnerability maps as a practical tool for the phases of planning and management of emergencies by international civil protection bodies and local authorities. Seismic vulnerability maps, in terms of vulnerability index and critical PGA values, provide a clear and unambiguous representation of the criticalities of a large scale territory. The overall procedure, leading to the definition of these instruments, has been adequately calibrated and may be repeated for the assessment of vulnerability of medium-small Mediterranean urban areas, characterized by certain repetitiveness of buildings typologies. Among the activities of the proposed procedure, the historical critical analysis of the territory and of its building typologies were first carried out. Subsequently the fast assessment of the seismic vulnerability of buildings and aggregates was performed by specific assessment forms (evaluation forms). Finally, a vulnerability model was chosen and calibrated through a deep experimental/numerical analysis of prototype buildings.

The overall finding that has emerged, based on the case study of the Lampedusaisland, has been in agreement with the predictions (which were made in the opening sections), in which a good general condition was recognized. The elements of the detected major criticality regarded essentially the presence of aggregates building with strong irregularities in elevation. These buildings reached in fact the highest levels of vulnerability. In accordance with the purposes stated, the major outputs obtained gave for the island of Lampedusaan univocal representation of the seismic risk for its urban centre area.

## CONFLICT OF INTEREST

The authors confirm that this article content has no conflict of interest.

## ACKNOWLEDGEMENTS

This study was supported by PO Italy – Malta 2007-2013. SIMIT Research Project: “Development of an integrated cross-border Italian-Maltese civil protection network”

## REFERENCES

- [1] D. Benedettini, and V. Petrini, "On seismic vulnerability of masonry buildings: proposal of an evaluation procedure", *L'industria delle costruzioni*, vol. 16, pp. 66-78, 1984.
- [2] F. Braga, M. Dolce, and D. Liberatore, "Fast and reliable damage estimations for optimal relief operations", In: *Proceedings of International Symposium on Earthquake Relief in Less Industrialized Areas, Zurich*. 1984, pp. 145-151.
- [3] P. Angeletti, A. Bellina, E. Guagenti, A. Moretti, and V. Petrini, "Comparison between vulnerability assessment and damage index, some results", In: *Proceedings of the 9<sup>th</sup> World Conference on Earthquake Engineering, Tokyo-Kyoto*. 1988, pp. 181-186.

- [4] S. Casolo, S. Grimaz, and V. Petrini, *Scala G.S.D.e.m. 93*, Internal Report. Dipartimento di Georisorse e Territorio, Università di Udine, 1993.
- [5] A. Martinelli, L. Corazza, A. Cherubini, M. Dolce, G. Di Pasquale, and V. Petrini, *Censimento di vulnerabilità degli edifici pubblici, strategici e speciali nelle regioni Abruzzo, Basilicata, Calabria, Campania, Molise, Puglia e Sicilia?* Relazione Generale.. Civil Protection Department: Rome, 1999.
- [6] M. Dolce, A. Masi, and C. Moroni, "Valutazione della vulnerabilità sismica di edifici scolastici della Provincia di Potenza", In: *Proceedings of XI National Congress L'ingegneria sismica in Italia*,. Genoa, 2004
- [7] M. Dolce, and C. Moroni, *La valutazione della vulnerabilità e del rischio sismico degli edifici pubblici le procedure VC (vulnerabilità C.A.) e VM (vulnerabilità muratura)*,. "Civil Protection Department", Potenza, 2005
- [8] M. Dolce, and A. Martinelli, "Inventario e vulnerabilità degli edifici pubblici e strategici dell'Italia centro-meridionale, vol", In: *II – Analisi di vulnerabilità e rischio sismico, INGV/GNDT*, Istituto Nazionale di geofisica e Vulcanologia/Gruppo Nazionale per la Difesa dai Terremoti, . L'Aquila, 2005.
- [9] P.G. Asteris, "On the structural analysis and seismic protection of historical masonry structures", *Open Constr. Build. Technol. J.*, vol. 2, pp. 124-133, 2008.  
[<http://dx.doi.org/10.2174/1874836800802010124>]
- [10] P.G. Asteris, M.P. Chronopoulos, C.Z. Chrysostomou, H. Varum, V. Plevris, N. Kyriakides, and V. Silva, "Seismic vulnerability assessment of historical masonry structural systems", *Eng. Struct.*, vol. 62-63, pp. 118-134, 2014.  
[<http://dx.doi.org/10.1016/j.engstruct.2014.01.031>]
- [11] "GNDT Gruppo Nazionale per la Difesa dai Terremoti", *Schede di 1° e 2° livello di vulnerabilità e di rilevamento del danno (edifici in c.a. e muratura)*,. 1994.
- [12] D.M. II. TT., 14/01/2008, Nuove norme tecniche per le costruzioni, 2008.
- [13] E. Guagenti, and V. Petrini, "Il caso delle vecchie costruzioni: verso una nuova legge danni-intensità", In: *Proceedings of the 4<sup>th</sup> Italian National Conference on Earthquake Engineering, Milan, Italy*, vol. 1. 1989, pp. 145-153.
- [14] V. Turnsek, and F. Cacovic, "Some experimental results on the strength of brick masonry walls", In: *Proceedings of the 2<sup>nd</sup> International Brick Masonry Conference, Stoke-on-Trent*. 1971, pp. 149-156.
- [15] E. Miranda, and V.V. Bertero, "Evaluation of strength reduction factors for earthquake resistant design", *Earthq. Spectra*, vol. 10, pp. 357-379, 1994.  
[<http://dx.doi.org/10.1193/1.1585778>]
- [16] T. Vidic, P. Fajfar, and M. Fishinger, "Consistent inelastic design spectra: strength and displacement: Evaluation of strength reduction factors for earthquake resistant design", *Earthq. Spectra*, vol. 10, pp. 357-379, 1994.  
[<http://dx.doi.org/10.1193/1.1585778>]

Received: June 30, 2015

Revised: August 15, 2015

Accepted: August 26, 2015

© Asteris et al.; License Bentham Open.

This is an open access article licensed under the terms of the Creative Commons Attribution-Non-Commercial 4.0 International Public License (CC BY-NC 4.0) (<https://creativecommons.org/licenses/by-nc/4.0/legalcode>), which permits unrestricted, non-commercial use, distribution and reproduction in any medium, provided the work is properly cited.